Int J Soc Robot (2013) 5:103–116
DOI 10.1007/s12369-012-0151-1

Fault-Tolerant Force in Human and Robot Cooperation

Hamid Abdi · Saeid Nahavandi · Zoran Najdovski · Anthony A. Maciejewski

Accepted: 18 April 2012 / Published online: 13 May 2012

Abstract Fault-tolerant solutions greatly benefit the dependability of robotic systems. This advantage is critical for robotic systems that perform in collaboration with humans. This work addresses the fault tolerance of robotic manipulators for cooperatively manipulating an object together with a human. Cooperation occurs for slow lifting or pushing of the object. Reconfiguration of the manipulator is performed to maintain the cooperative force level despite the occurrence of robot joint failures. We present several strategies that are investigated for optimally maintaining the required force level for human-robot task cooperation. For each strategy, a reconfiguration control law is introduced that optimises the fault tolerance of the maintained force level. Three case studies are introduced to validate the proposed reconfiguration laws,demonstrating that this approach results in an optimal fault-tolerant force in human-robot cooperation.

Keywords Human-robot cooperation · Fault-tolerant robot · Safety · Reliability

1 Introduction

Human-robot collaboration has recently received increasing interest within the robotics community [1, 2]. Within this collaboration, for the robotic system to be dependable, a high level of reliability and safety must be achieved [3]. Robotic systems are being specifically designed and developed to operate within human proximity. Such examples are a work partner robot, which assists humans [4], astronauts [5], surgeons [6], the elderly, and also people with disabilities [2, 7–9]. Improving the performance of this collaboration can greatly benefit robot dependability, and consequently increase human task accuracy and efficiency.

All aspects of human-robot cooperation (HRC) are important [10], including fault tolerance. Fault tolerance is a significant factor due to improving the dependability of the robotic system [10, 11]. In social robotics, the level of dependability is a critical component of the robotic system for meeting the specific safety requirements. The subject of safety plays a significant role when it is crucial to complete the required task even in the event of partial failure of the robotic system [11–13]. In addition, without fault tolerance strategies, the dependability of the robot is vulnerable, and failure of the robot can result in non-desired behavior throughout its process.

Current research that addresses HRC and human-robot interaction (HRI) can be classified into the three categories, physical, emotional and safety [14–16]. With presently little focus on the physical category of HRC, existing work centres on the area of manipulation, and does not lend itself to properties such as fault tolerance. For example, Kosuge et al. [17], utilise a double arm robot (Mr Helper), to support an object's weight, where the human can apply a force to the object in order to move it. Such a mechanism fails to support the object weight in the case of joint failure of the robot.

Using impedance control methods, a force control HRC approach has been realised by Tsumugiwa [18] and Takubo [19]. By means of this method,other implementations and applications of force control HRC have also been introduced [9, 20–24]. While this work makes significant contribution to human-robot cooperation, it does not address recovery

H. Abdi · S. Nahavandi · Z. Najdovski
Center for Intelligent Systems Research, Deakin University, Geelong Waurn Ponds Campus, Victoria 3217, Australia

H. Abdi (✉) · A.A. Maciejewski
Electrical and Computer Engineering Department, Colorado State University, Fort Collins, CO 80523, USA
e-mail: hamid.abdi@deakin.edu.au

from failure of the robotic systems, and completing its required process.Consequently, if the robot's joint fails, the desired cooperation will no longer be maintained,which can result in serious damage or injury.

Fault-tolerant HRC is advantageous to increase the level of robot reliability and ensure that tasks are completed despite joint failure.The fault-tolerant force approach for human-robot cooperation [13] demonstrates two fault tolerance strategies based on the reconfiguration of the robot joint torques, and the human's force. The present work extends on this by introducing the general form of the strategies.

This paper is organized as follows: Sect. 2 indicates the kinematics and dynamics of manipulators subject to locked joint failures. Section 3 obtains the force-jump due to the locked joint failures in human and robot cooperation. In Sect. 4, six post failure cooperation strategies to minimize the force-jump are proposed. Three case studies are demonstrated in Sects. 5–7. Finally, the concluding remarks are presented in Sect. 7.

2 Kinematics of Redundant Manipulators

2.1 Notation Hints

1. In all formulas, bold uppercase letters are matrices, bold lowercase letters are vectors, and lower case letters are scalars.
2. There are three notations for forces. The forces prior to the failure $\mathbf{f}$, at failure time $\hat{\mathbf{f}}$, post failure forces $\tilde{\mathbf{f}}$.
3. The star symbol for parameters indicates the maximum bound,for example $\mathbf{f}^*$ is the bound of force.

2.2 Assumptions

There are three assumptions, including slow moving or stationary force tasks, small operational workspace, and locked joint failure. The slow moving or stationary assumption is because of the safety of the human who is in proximity to the robot and collaborates with the robot. The second assumption is because the robot moves slowly or is stationary, therefore the task is in a small part of the robot workspace. One example of this can be surgical robots as they move in a small operation workspace with slow velocity.

Another assumption is that the paper addresses the locked-joint failures of the robot. Although the presented method is not applicable for other failures, it is possible to consider a mechanical brake in order to lock the joints. In this case, the proposed method of this paper will be applicable for other types of joint failures.

2.3 Kinematics of Serial Manipulators

Forward kinematics of serial manipulators relates joint variables to the EEF positional variables through the forward kinematic equation

$$\mathbf{x} = \mathbf{k}(\mathbf{q}) \tag{1}$$

where $\mathbf{q} = [q_1\ q_2\ \cdots\ q_n]^T \in R^n$ are joint variables, $\mathbf{x} = [x_1\ x_2\ \cdots\ x_m]' \in R^m$ are positional variables, and $\mathbf{k}(\cdot) : R^n \to R^m$.

The configuration space (C-space) or joint space is defined by $\mathbf{q}$ and the workspace is defined by $\mathbf{x}$. The dimension of the C-space is n and the dimension of the workspace is m. For positional manipulators in 3D space $m = 3$ and in 2D space $m = 2$. In the planar case (2D), it is possible to consider $m = 3$ where the z-component is always fixed.The fault tolerance is more likely to be achieved in a redundant manipulator where $n > m$. The degree of redundancy in non-singular configuration is $r = n - m$.

2.4 Velocity and Force Equations and Locked Joint Failures

The EFF translational velocity equation is

$$\dot{\mathbf{x}} = \mathbf{J}\dot{\mathbf{q}} \tag{2}$$

where $\mathbf{J} \in R^{3\times n}$ is the analytic Jacobian matrix defined by $\mathbf{J} = \frac{\partial \mathbf{k}(\mathbf{q})}{\partial \mathbf{q}}$.

The EEF force $\mathbf{f}$ is related to the joint-torques by

$$\boldsymbol{\tau} = \mathbf{J}^T\mathbf{f} \tag{3}$$

where $\boldsymbol{\tau} = [\tau_1\ \tau_2\ \cdots\ \tau_n]^T$ is torque vector.

For the manipulator in a non-singular configuration, the EEF force is obtained by

$$\mathbf{f} = \left(\mathbf{J}^T\right)^{\dagger}\boldsymbol{\tau} + \left(\mathbf{I} - \left(\mathbf{J}^T\right)^{\dagger}\mathbf{J}^T\right)\mathbf{z} \tag{4}$$

where $\mathbf{I} \in R^{m\times m}$ is an identity matrix, $(\mathbf{J}^T)^{\dagger}$ is the pseudo inverse of $\mathbf{J}^T$, and $\mathbf{z} \in R^m$ is an arbitrary vector.

This arbitrary vector is mapped into the null space of $\mathbf{J}^T$ by the null space projection matrix $(\mathbf{I} - (\mathbf{J}^T)^{\dagger}\mathbf{J}^T)$. The pseudo inverse of $\mathbf{J}^T$ at the non-singular configuration is defined by the regular inverse, left inverse,or right inverse as shown in Appendix A.

2.5 Model of Locked Joint Failures

To model the EEF force subject to a locked joint failure, we assume

$$\mathbf{A} = \left(\mathbf{J}^T\right)^{\dagger} \tag{5}$$

where $\mathbf{A} = [\mathbf{a}_1\ \cdots\ \mathbf{a}_{k-1}\ \mathbf{a}_k\ \mathbf{a}_{k+1}\ \cdots\ \mathbf{a}_n]$ and $\mathbf{a}_k$ is the kth column of $\mathbf{A}$.

Using the above convention, as the force in (4) can be written by

$$\mathbf{f} = \sum_{i=1}^{n} \mathbf{a}_i \boldsymbol{\tau}_i + \left(\mathbf{I} - \left(\mathbf{J}^T\right)^{\dagger}\mathbf{J}^T\right)\mathbf{z} \tag{6}$$

Each column of $\mathbf{A}$ indicates the contribution of the corresponding joint to the EEF force. Therefore, when a locked joint failure occurs in the kth joint, the joint stops contributing and the force can be modeled by eliminating $\mathbf{a}_k\boldsymbol{\tau}_k$ from (6)

$$\hat{\mathbf{f}} = \sum_{i=1}^{n} \mathbf{a}_i \boldsymbol{\tau}_i - \mathbf{a}_k\boldsymbol{\tau}_k + \left(\mathbf{I} - \left(\mathbf{J}^T\right)^{\dagger}\mathbf{J}^T\right)\mathbf{z} \tag{7}$$

By using the convention of reduced matrices and vectors (presented in Appendix B), the force at failure time is

$$\hat{\mathbf{f}} = {}^k\mathbf{A}\,{}^k\boldsymbol{\tau} + \left(\mathbf{I} - \left(\mathbf{J}^T\right)^{\dagger}\mathbf{J}^T\right)\mathbf{z} \tag{8}$$

where ${}^k\mathbf{A}$ is the kth reduced matrix and ${}^k\boldsymbol{\tau} \in R^{n-1}$ is the kth reduced vector.

2.6 Stationary or Slow Pushing or Lifting Force

The dynamic equation of the manipulator when an EEF force ${}_m\mathbf{f}$ is required is

$$\mathbf{M}(\mathbf{q})\ddot{\mathbf{q}} + \mathbf{V}(\mathbf{q},\dot{\mathbf{q}})\dot{\mathbf{q}} + \mathbf{g}(\mathbf{q}) + \mathbf{J}^T{}_m\mathbf{f} = \boldsymbol{\tau} \tag{9}$$

where $\mathbf{M}(\mathbf{q})$ is the inertia matrix, $\mathbf{V}(\mathbf{q},\dot{\mathbf{q}})\dot{\mathbf{q}}$ is Coriolis-centrifugal term and $\mathbf{g}(\mathbf{q})$ is the gravity term, $\boldsymbol{\tau}$ is the torque and $\mathbf{J}^T{}_m\mathbf{f}$ in the left side is the torque required to apply EEF force ${}_m\mathbf{f}$.

If an external force is applied to the robot's EEF, then $\mathbf{J}^T{}_m\mathbf{f}$ is considered in the right side. However, in our case, we don't apply a force to the EEF, therefore the term $\mathbf{J}^T{}_m\mathbf{f}$ is not in the left side. In this paper, the robot applies force ${}_m\mathbf{f}$ by its EEF to an external load, therefore the term $\mathbf{J}^T{}_m\mathbf{f}$ is considered in the right side of the (9). This is because the required torque is for the motion of the robot which is defined by $\mathbf{M}(\mathbf{q})\ddot{\mathbf{q}} + \mathbf{V}(\mathbf{q},\dot{\mathbf{q}})\dot{\mathbf{q}} + \mathbf{g}(\mathbf{q})$ plus for the EEF force ${}_m\mathbf{f}$ which is defined by $\mathbf{J}^T{}_m\mathbf{f}$.

If the manipulator is stationary or moves slowly $\dot{\mathbf{q}}, \ddot{\mathbf{q}} \approx 0$, then (9) is simplified to $\mathbf{g}(\mathbf{q}) + \mathbf{J}^T{}_m\mathbf{f} = \boldsymbol{\tau}$. Therefore, the required torque is the torque due to the gravity and the torque to apply the EEF force. Hence $\mathbf{g}(\mathbf{q})$ is known, therefore the required torque is obtained by adding $\mathbf{g}(\mathbf{q})$ to $\mathbf{J}^T{}_m\mathbf{f}$.

2.7 Fault-Tolerant Force for HRC

Assume a robot and human are providing a cooperative force for lifting objects as shown in Fig. 1. The total-force is

$$\mathbf{f} = {}_m\mathbf{f} + {}_h\mathbf{f} \tag{10}$$

where ${}_m\mathbf{f}$ is the manipulator force and ${}_h\mathbf{f}$ is the human force.

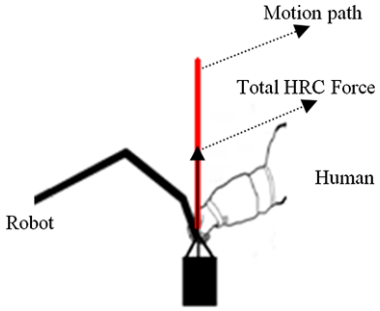

Fig. 1 Human-robot force cooperation in load lifting application

If a locked joint failure occurs in the manipulator, then EEF force changes [25] by the force-jump $\Delta_m\mathbf{f}$. Accordingly, the total-force will result to ${}_m\mathbf{f} + {}_h\mathbf{f} + \Delta_m\mathbf{f}$ and the total-force-jump is $\Delta\mathbf{f} = \Delta_m\mathbf{f}$.

The present paper aims to address the following questions:

1. How the manipulator and the human can tolerate the failure or minimize the total-force-jump?
2. What are the strategies for reconfiguring the human force and the manipulator torque?
3. What are the conditions to provide a zero force-jump?

These questions are more challenging when considering: (a) the optimality of the post failure cooperation of the human and the manipulator, (b) the physical limitation of the human force, and (c) the physical limitation of the faulty manipulator [14].

3 Force-Jump in Human and Robot Cooperation

3.1 Locked Joint Failure via Perturbation Method

When the kth joint of the manipulator fails, then the force equation is perturbed

$${}_m\hat{\mathbf{f}} = (\mathbf{A} + \Delta\mathbf{A})(\boldsymbol{\tau} + \Delta\boldsymbol{\tau}) + \left(\mathbf{I} - \left(\mathbf{J}^T\right)^{\dagger}\mathbf{J}^T\right)\mathbf{z} \tag{11}$$

where $\Delta\boldsymbol{\tau}$ is the torque jump, $\Delta\mathbf{A}$ is matrix perturbation and $\Delta_m\hat{\mathbf{f}}$ is the force-jump which is obtained as

$$\Delta_m\hat{\mathbf{f}} = (\mathbf{A} + \Delta\mathbf{A})\Delta\boldsymbol{\tau} + \Delta\mathbf{A}\boldsymbol{\tau} \tag{12}$$

where $\Delta\boldsymbol{\tau} = [0 \ \cdots \ 0 \ -\tau_{k-1} \ 0 \ \cdots \ 0]^T$ and $\Delta\mathbf{A} = [0 \cdots 0 \ -\mathbf{a}_k \ 0 \cdots 0]$.

It is easy to check that $(\mathbf{A} + \Delta\mathbf{A})\Delta\boldsymbol{\tau} = 0$ and $\Delta\mathbf{A}\boldsymbol{\tau} = -\mathbf{a}_k\tau_k$. This results in $\Delta_m\hat{\mathbf{f}} = -\mathbf{a}_k\tau_k$. Knowing that the force of the human at failure time is ${}_h\hat{\mathbf{f}} = {}_h\mathbf{f}$. Therefore, the total-force at failure time is $\hat{\mathbf{f}} = {}_m\hat{\mathbf{f}} + {}_h\hat{\mathbf{f}}$ and the total-force-jump is $\Delta\hat{\mathbf{f}} = \mathbf{f} - \hat{\mathbf{f}} = \mathbf{a}_k\tau_k$.

3.2 Fault-Tolerant Force via Reconfiguration

The HRC aims to provide a total-force for a task. These two forces should not oppose each other and they are preferred to be in the same or close directions. When a fault occurs, then a reconfiguration is required to minimize the post failure force-jump. This requires reconfiguration of the manipulator's torque and humans force. After the reconfiguration, the post failure human force is ${}_h\tilde{\mathbf{f}}$ and manipulators EEF force is ${}_m\tilde{\mathbf{f}}$. The reconfiguration of the manipulator's force is performed by adding a reconfiguration torque $\mathbf{u}$, to the remaining healthy joints

$$ {}_m\tilde{\mathbf{f}} = (\mathbf{A} + \Delta\mathbf{A})(\boldsymbol{\tau} + \Delta\boldsymbol{\tau} + \mathbf{u}) + \left(\mathbf{I} - \left(\mathbf{J}^T\right)^{\dagger}\mathbf{J}^T\right)\mathbf{z} \tag{13} $$

Note that $\mathbf{u}$ should have a zero value in its kth row because the kth joint is locked

$$ \mathbf{u} = \begin{bmatrix} u_1 \cdots u_{k-1}\ 0\ u_{k+1} \cdots u_n \end{bmatrix}^T \in R^n \tag{14} $$

Using the convention of reduced matrices

$$ {}_m\tilde{\mathbf{f}} = {}_m\mathbf{f} + {}^k\mathbf{A}\,{}^k\mathbf{u} - \mathbf{a}_k\tau_k \tag{15} $$

where ${}^k\mathbf{u} = [u_1 \ \cdots \ u_{k-1}\ u_{k+1} \ \cdots \ u_n]^T \in R^{n-1}$.

The total-force-jump after reconfiguration is $\Delta\tilde{\mathbf{f}} = \mathbf{f} - \tilde{\mathbf{f}}$ where $\tilde{\mathbf{f}} = {}_m\tilde{\mathbf{f}} + {}_h\tilde{\mathbf{f}}$ and force-jump will be

$$ \Delta\tilde{\mathbf{f}} = -{}^k\mathbf{A}\,{}^k\mathbf{u} + \mathbf{a}_k\tau_k + {}_h\mathbf{f} - {}_h\tilde{\mathbf{f}} \tag{16} $$

3.3 Optimal Fault Tolerance

Optimal fault tolerance is defined based on the minimization of the post failure total-force-jump.

$$ \underset{\mathbf{u},{}_h\tilde{\mathbf{f}}}{\text{Min}} \|\Delta\tilde{\mathbf{f}}\|^2 \tag{17} $$

The constraints associated to (17) include: (a) the bounds of the human force and (b) the bounds of the manipulator joint torque.

When ${}_h\mathbf{f}^*$ is a 3 dimensional vector showing the maximum human force in x, y and z directions in the 3D space for a particular configuration of the human, the constraints of the maximum human force are:

$$ -{}_h\mathbf{f}^* < {}_h\tilde{\mathbf{f}} < {}_h\mathbf{f}^* \tag{18} $$

Similarly, when ${}^k\boldsymbol{\tau}^* \in R^{n-1}$ is the maximum torque of the healthy joints, the constraints of the torques are

$$ -{}^k\boldsymbol{\tau}^* < {}^k\boldsymbol{\tau} + {}^k\mathbf{u} < {}^k\boldsymbol{\tau}^* \tag{19} $$

If the manipulator works in a 3D space, then there are $2n+4$ constraints associated with (18)–(19) and there are $n+2$ variables associated with ${}^k\mathbf{u} \in R^{n-1}$ and ${}_h\tilde{\mathbf{f}} \in R^3$. However, for 2D planar manipulators, there are $2n+2$ constraints and $n+1$ variables.

4 Strategy for Optimal Fault Tolerance

4.1 General Strategy for Optimal Fault Tolerance

The constrained minimization can be solved via various iterative techniques. This is a general way for fault tolerance. This strategy will be later demonstrated in case study 1. For this strategy, it is observed that there is no appropriate control over the minimum force-jump and the post failure cooperation of the human and robot. The fact is that the fault tolerance is very sensitive to the initial guess and the optimization technique. The lack of appropriate control on the minimum force-jump and post failure cooperation motivates developing specific strategies. The specific strategies are expected to provide a better control on the post failure cooperation and specify the minimum force-jump.

4.2 Specific Strategies for Optimal Fault Tolerance and Minimum Force-Jump

Five specific strategies are identified which are introduced and formulated in this section. We categorise them into non-cooperative and cooperative fault tolerance strategies.

4.2.1 Non-cooperative Strategies

Strategy I: In this strategy, the manipulator is responsible for its fault tolerance and the human would not contribute for tolerating the fault. Therefore, the post failure human force remains as equal to that prior to failure ${}_h\tilde{\mathbf{f}} = {}_h\mathbf{f}$. And after the torque reconfiguration of the manipulator ${}_m\tilde{\mathbf{f}} = {}_m\mathbf{f} + {}^k\mathbf{A}\,{}^k\mathbf{u} - \mathbf{a}_k\tau_k$.

Then, the post failure total-force-jump is obtained by

$$ \Delta\tilde{\mathbf{f}} = -{}^k\mathbf{A}\,{}^k\mathbf{u} + \mathbf{a}_k\tau_k \tag{20} $$

The minimum total-force-jump is achieved by using the pseudo inverse method [26, 27] by

$${}^k\mathbf{u}^{\text{opt}} = \left({}^k\mathbf{A}\right)^{\dagger}\mathbf{a}_k\tau_k \tag{21}$$

By using the optimal joint-torque reconfiguration, a minimum total-force-jump is obtained by

$$ \Delta\tilde{\mathbf{f}}_{\min} = \left(\mathbf{I} - {}^k\mathbf{A}\left({}^k\mathbf{A}\right)^{\dagger}\right)\mathbf{a}_k\tau_k \tag{22} $$

The matrix $(\mathbf{I} - {}^k\mathbf{A}({}^k\mathbf{A})^{\dagger})$ is the null space projection matrix that gives (22), a nice physical interpretation. It says that the minimum force-jump is the projection of $\mathbf{a}_k\tau_k$ into the null space of ${}^k\mathbf{A}$. Knowing that $\mathbf{a}_k\tau_k$ is the lost part of the force due to the failure, therefore, if this force does not have any projection into null space of ${}^k\mathbf{A}$ or if the null space is zero, then the post failure total-force-jump is zero.

Strategy II: In this strategy, the manipulator does not contribute to the fault tolerance. Therefore, the whole responsibility of fault tolerance is with the human. This can be justified where the user aims to prevent any further failure to the

manipulator. In this strategy ${}^k\mathbf{u}$ would be a zero vector and the post failure manipulator force is

$${}_m\tilde{\mathbf{f}} = {}_m\mathbf{f} - \mathbf{a}_k\tau_k \tag{23}$$

The force-jump of the manipulator is $\mathbf{a}_k\tau_k$. Therefore, the required post failure human force is

$${}_h\tilde{\mathbf{f}} = {}_h\mathbf{f} + \mathbf{a}_k\tau_k \tag{24}$$

For this strategy, the total-force-jump would be zero if the human force remains in its bound $-{}_h\mathbf{f}^* < {}_h\tilde{\mathbf{f}} < {}_h\mathbf{f}^*$. However, if the required post failure human force is out of this bound, then the force-jump depends on the difference of ${}_h\tilde{\mathbf{f}}$ and the bounds.

4.2.2 Cooperative Strategies

In this category of the strategies, three cooperative strategies are proposed. These strategies are based on different ways of distributing the force-jump between the faulty manipulator and the human.

Strategy III: This strategy is a cooperative form of strategy I, where the main responsibility of the fault tolerance is with the manipulator. Therefore, the manipulator maximally compensates the force-jump similar to that of strategy I. The remainder of the force-jump which is shown by (22) is assigned to the human. Therefore, the manipulator optimally compensates the force-jump, and the reconfiguration joint-torque is obtained by

$${}^k\mathbf{u}^{\text{opt}} = \left({}^k\mathbf{A}\right)^{\dagger}\mathbf{a}_k\tau_k \tag{25}$$

The remaining force-jump $(I - {}^k\mathbf{A}({}^k\mathbf{A})^{\dagger})\mathbf{a}_k\tau_k$ needs to be provided by the human. Therefore the required post failure human force is

$${}_h\tilde{\mathbf{f}} = {}_h\mathbf{f} + \left(\mathbf{I} - {}^k\mathbf{A}\left({}^k\mathbf{A}\right)^{\dagger}\right)\mathbf{a}_k\tau_k \tag{26}$$

In strategy III, the total-force-jump is zero if the required post failure human force is in the bound of $-{}_h\mathbf{f}^* < {}_h\tilde{\mathbf{f}} < {}_h\mathbf{f}^*$. If it is not in this bound, then the force-jump depends on the difference between ${}_h\tilde{\mathbf{f}}$ and the bound.

Strategy IV: This strategy is a cooperative form of strategy II where the main responsibility of the fault tolerance is with the human. Therefore, the human maximally covers the force-jump. If any force remains which is out of the human's capability, then it would be assigned to the faulty manipulator.

The force of the human is required to be ${}_h\tilde{\mathbf{f}} = {}_h\mathbf{f} + \mathbf{a}_k\tau_k$ that was introduced by (24). If the human is unable to apply this level of force, then the difference between the assigned human force and the human's force bound is assigned to the manipulator.

Note that the force is a vector, therefore, if any component of the human force is in the bound, the force-jump associated to the component is zero, but if not, the difference is obtained. For example, if the required post failure human force is ${}_h\mathbf{f} = [-25_N\ 10_N\ 35_N]^T$ and the maximum human force is ${}_h\mathbf{f}^* = [20_N\ 20_N\ 20_N]^T$ then the human force will be ${}_h\tilde{\mathbf{f}} = [-20_N\ 10_N\ 20_N]^T$ and the remaining force-jump is $[-5_N\ 0_N\ 15_N]^T$. The manipulator changes its joint-torque to optimally cover the remaining force-jump. If the remaining force-jump is depicted by ${}_r\mathbf{f}$ then the required change in the manipulator force is

$${}_m\hat{\mathbf{f}} - {}_m\tilde{\mathbf{f}} = {}_r\mathbf{f} - {}^k\mathbf{A}\,{}^k\mathbf{u} \tag{27}$$

Consequently, the optimal post failure joint-torque reconfiguration is obtained by

$${}^k\mathbf{u}^{\text{opt}} = -\left({}^k\mathbf{A}\right)^{\dagger}{}_r\mathbf{f} \tag{28}$$

Using this joint-torque, the minimum total-force-jump will be

$$\Delta\tilde{\mathbf{f}}_{\min} = \left(\mathbf{I} - {}^k\mathbf{A}\left({}^k\mathbf{A}\right)^{\dagger}\right){}_r\mathbf{f} \tag{29}$$

The minimum total-force-jump is the projection of ${}_r\mathbf{f}$ into the null space of ${}^k\mathbf{A}$.

Strategy V: In this strategy, the fault is tolerated using a decision-making process. A decision maker assigns the force for the post failure cooperation for the human and the robot. Optimal decision making for assigning post failure force to the robot and the human requires further research. For this strategy, we assume that the decision maker is known. In this case, the decision maker defines two arbitrary matrices ${}_m\mathbf{W}$ and ${}_h\mathbf{W}$ where ${}_m\mathbf{W} + {}_h\mathbf{W} = \mathbf{I}$ and ${}_m\mathbf{W}$ is to assign the post failure force for the robot and ${}_h\mathbf{W}$is to assign the post failure force for the human. Then, the total-force-jump is divided into two parts

$$\Delta\hat{\mathbf{f}} = ({}_m\mathbf{W} + {}_h\mathbf{W})\Delta\hat{\mathbf{f}} = {}_m\mathbf{W}\Delta\hat{\mathbf{f}} + {}_h\mathbf{W}\Delta\hat{\mathbf{f}} \tag{30}$$

where ${}_m\mathbf{W}\Delta\hat{\mathbf{f}}$ is the force assigned to the manipulator, and ${}_h\mathbf{W}\Delta\mathbf{f}$ is assigned to the human.

Therefore, the required post failure human force is

$${}_h\tilde{\mathbf{f}} = {}_h\mathbf{f} + {}_h\mathbf{W}\mathbf{a}_k\tau_k \tag{31}$$

The required post failure manipulator force is

$${}_m\tilde{\mathbf{f}} = {}_m\hat{\mathbf{f}} + {}_m\mathbf{W}\mathbf{a}_k\tau_k \tag{32}$$

Knowing that ${}_m\tilde{\mathbf{f}} = {}_m\mathbf{f} + {}^k\mathbf{A}\,{}^k\mathbf{u} - \mathbf{a}_k\tau_k$ and ${}_m\hat{\mathbf{f}} = {}_m\mathbf{f} - \mathbf{a}_k\tau_k$ then, the reconfiguration is

$${}^k\mathbf{A}\,{}^k\mathbf{u} = {}_m\mathbf{W}\mathbf{a}_k\tau_k \tag{33}$$

The optimal joint-torque to minimise the post failure force-jump is

$${}^k\mathbf{u}^{\text{opt}} = \left({}^k\mathbf{A}\right)^{\dagger}{}_m\mathbf{W}\mathbf{a}_k\tau_k \tag{34}$$

The optimal post failure force of the manipulator is

$${}_m\tilde{\mathbf{f}} = {}_m\mathbf{f} + \left({}^k\mathbf{A}\left({}^k\mathbf{A}\right)^{\dagger}{}_m\mathbf{W} - \mathbf{I}\right)\mathbf{a}_k\tau_k \tag{35}$$

Then, the optimal post failure total-force is obtained by

$$\tilde{\mathbf{f}} = \mathbf{f} + \left({}^{k}\mathbf{A}\left({}^{k}\mathbf{A}\right)^{\dagger}{}_{m}\mathbf{W} - \mathbf{I}\right)\mathbf{a}_k\tau_k + {}_{h}\mathbf{W}\mathbf{a}_k\tau_k \tag{36}$$

Finally, the minimum post failure total-force-jump is

$$\Delta\tilde{\mathbf{f}}_{\min} = \left(\mathbf{I} - {}^{k}\mathbf{A}\left({}^{k}\mathbf{A}\right)^{\dagger}\right)_{m}\mathbf{W}\mathbf{a}_k\tau_k \tag{37}$$

In this strategy, if the human is capable of providing the assigned force ${}_{h}\tilde{\mathbf{f}} = {}_{h}\mathbf{f} + {}_{h}\mathbf{W}\mathbf{a}_k\tau_k$ or the assigned human force is in the bound then (37) gives the following conditions of a zero force-jump.

1. When
$$\left(\mathbf{I} - {}^{k}\mathbf{A}\left({}^{k}\mathbf{A}\right)^{\dagger}\right)_{m}\mathbf{W} = \mathbf{0} \tag{38}$$
2. When $\mathbf{a}_k\tau_k$ belongs to the null space of
$$\left(\mathbf{I} - {}^{k}\mathbf{A}\left({}^{k}\mathbf{A}\right)^{\dagger}\right)_{m}\mathbf{W} \tag{39}$$
3. When $\mathbf{a}_k\tau_k = 0$

If the human is capable of providing the assigned force, then the minimum total-force-jump only depends on the projection of the manipulator's assigned force to the null space of the manipulator.

The conditions of a zero force-jump is useful to define values for ${}_{m}\mathbf{W}$ and ${}_{h}\mathbf{W}$ by the decision maker.

4.3 Consistency Between the Proposed Strategies

To indicate the consistency between the proposed strategies, here we deal with strategy 5. In this strategy, if the whole force is assigned to the manipulator, then ${}_{m}\mathbf{W} = \mathbf{I}$ and ${}_{h}\mathbf{W} = \mathbf{0}$. Therefore ${}_{h}\tilde{\mathbf{f}} = {}_{h}\mathbf{f}$ and ${}^{k}\mathbf{u}^{\text{opt}} = ({}^{k}\mathbf{A})^{\dagger}\mathbf{a}_k\tau_k$ that are obtained by substitution of ${}_{m}\mathbf{W} = \mathbf{I}$ and ${}_{h}\mathbf{W} = \mathbf{0}$ in (31) and (34). These results are consistent with those in strategy I.

On the other hand, if one requires that the force is fully compensated by the human then ${}_{m}\mathbf{W} = \mathbf{0}$ and ${}_{h}\mathbf{W} = \mathbf{I}$ simply substituting ${}_{m}\mathbf{W} = \mathbf{0}$ into (31)–(32), results in ${}_{h}\mathbf{f} + \mathbf{a}_k\tau_k$ and ${}_{m}\tilde{\mathbf{f}} = {}_{m}\hat{\mathbf{f}}$. Which are consistent with the results of strategy II.

Interestingly, the five proposed strategies are consistent with each other, because they have been built on each other. This consistency is observed between the ways that the strategies are formulated and between the results of the assigned force to the human and the manipulator. For example, consider the consistency between (25) in strategy III, and (21) in strategy I, and the similar observation between strategy IV and strategy II. Despite the observed consistency, the strategies work differently because in each strategy a key difference exists. This makes it independent from the other strategies.

This section proposed one general strategy and five specific strategies. From these six strategies, strategy III and IV have been already published by the authors in [13]. In the following sections, three case studies are presented to demonstrate the fault-tolerant for HRC.

Table 1 D-H parameters of the 3DoF planar manipulator

Joint No.	s_i (m)	d_i (m)	α_i (rad)	θ_i
1	0.05	0.50	0	θ_1
2	0.05	0.40	0	θ_2
3	0.05	0.30	0	θ_3

Table 2 Configuration of the manipulator prior to the failure time

Joint No.	Joint angle (deg)	Joint-torque (N m)	EEF Force (N)
1	25	−22.73	${}_{m}\mathbf{f} = \begin{bmatrix} 45_N \\ 70_N \\ 0_N \end{bmatrix}$
2	90	−44.94	
3	80	−16.79	

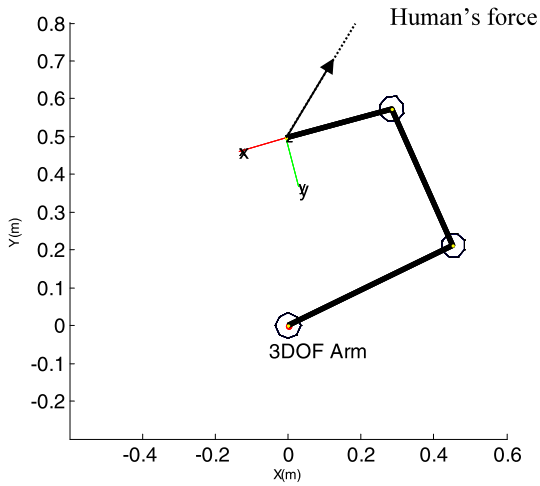

Fig. 2 Manipulator configuration and human force, the *arrow* shows the direction of the human force

5 Case Study 1—Test of the Generalized Strategy

A force is provided by a 3DoF planar manipulator and human. This case study considers a stationary force for pressing against a surface.

5.1 Case Study 1—Parameters

Table 1 presents the Denavit Hartenberg (D-H) parameters of a 3DoF planar manipulator. Table 2 shows the configuration parameters of the manipulator at failure time,and includes joint angles and torques. The manipulator configuration is depicted in Fig. 2. The robot is modeled in Matlab Robotics Toolbox [28]. From the given joint-torques, the EEF force prior to the failure is ${}_{m}\mathbf{f} = [45_N\ 70_N\ 0_N]^T$, a human and the manipulator are cooperatively providing the total-force of $\mathbf{f} = [50_N\ 80_N\ 0_N]^T$ where the human force prior to fault is ${}_{h}\mathbf{f} = [5_N\ 10_N\ 0_N]^T$ shown with an arrow. It is assumed that the maximum human force is

${}_h\mathbf{f}^* = [20_N \ 20_N \ 0_N]^T$ and the maximum torque is $\boldsymbol{\tau}^* = [100_{N.m} \ 100_{N.m} \ 100_{N.m}]^T$.

At this configuration, the positional Jacobian matrix of the manipulator is

$$\mathbf{J} = \begin{bmatrix} -0.4962 & -0.2849 & 0.0776 \\ -0.0057 & -0.4588 & -0.2898 \end{bmatrix} \tag{40}$$

The z-components of the Jacobian matrix, the human force, and the manipulator forces are eliminated because of the 2D application and $\mathbf{A} = (\mathbf{J}^T)^\dagger$

$$\mathbf{A} = \begin{bmatrix} -1.6947 & -0.3839 & 0.6410 \\ 0.6196 & -1.4131 & -1.2255 \end{bmatrix} \tag{41}$$

If a locked joint fault occurs in the second joint, then, the 2-nd reduced matrix of $\mathbf{A}$ is

$${}^2\mathbf{A} = \begin{bmatrix} -1.6947 & 0.6410 \\ 0.6196 & -1.2255 \end{bmatrix} \tag{42}$$

The parameters that are used later include

$$\mathbf{a}_2 = \begin{bmatrix} -0.3839 \\ -1.4131 \end{bmatrix}, \qquad {}^2\boldsymbol{\tau} = \begin{bmatrix} 13.03_{N.m} & 21.00_{N.m} \end{bmatrix}^T,$$

$\tau_2 = 43.59_{N.m}$ and ${}_h\mathbf{f} = [5_N \quad 10_N]^T$.

The force-jump of the manipulator is $\Delta_m\mathbf{f} = -\mathbf{a}_2\tau_2$ that is $\Delta_m\mathbf{f} = [-17.25_N \ -63.50_N]^T$. The force of the manipulator at fault time is ${}_m\hat{\mathbf{f}} = [27.75_N \ 6.50_N]^T$.

This case study aims to test the general strategy. In this strategy, the torque reconfiguration command is for the first and third joints ${}^2\mathbf{u} = [u_1 \ u_3]^T$, and the post failure human force is ${}_h\tilde{\mathbf{f}} = [{}_h\tilde{f}_1 \ {}_h\tilde{f}_2]^T$. The post failure total-force-jump is $\Delta\tilde{\mathbf{f}} = {}^2\mathbf{A}^2\mathbf{u} - \mathbf{a}_2\tau_2 + {}_h\mathbf{f} - {}_h\tilde{\mathbf{f}}$ the norm of the force-jump is $\|\Delta\tilde{\mathbf{f}}\|^2 = \Delta\tilde{\mathbf{f}}^T\Delta\tilde{\mathbf{f}}$. We have minimized $\|\Delta\tilde{\mathbf{f}}\|^2$ by using "*Optimtool*" of Matlab.

5.2 Case Study 1—Optimization Results

The results of the constrained optimization of $\|\Delta\tilde{\mathbf{f}}\|^2$ are shown in Table 3 for two different executions. The table includes the post failure torque reconfiguration command and the post failure human force. The force-jump for each run is also shown in the last row of the table indicating that the failure was tolerated in both runs. The two runs are with different initial guess and two different solver of "*Optimtool*". The solvers are *active set* and *interior point*.

5.3 Discussion

The proposed method for minimum force-jump indicated was demonstrated to be efficient for fault tolerance. The minimum force-jump was achieved in the both runs. From the results, it is observed that there is no control over the post failure cooperation of the human and the robot. The fact is that the fault tolerance is very sensitive to the initial guess and the optimization technique.

Table 3 Two runs of the optimization routine

Variables	Run 1	Run 2
u_1	−32.87 N m	−38.83 N m
u_3	−67.12 N m	−74.08 N m
${}_h\tilde{f}_1$	9.57 N	3.94 N
${}_h\tilde{f}_2$	11.61 N	6.77 N
$\|\Delta\tilde{\mathbf{f}}\|$	2.09e−4 N	4.016e−7 N

6 Case Study II—Test of the Specific Strategies

6.1 Case Study Parameters

A 3DoF planar manipulator of the previous case study is used in this case study with the same parameters. The five proposed specific strategies presented in Sect. 4 are deployed here for obtaining the fault tolerance force for the HRC illustrated in Fig. 1.

6.2 Tests of the Non-cooperative Strategies

Test of Strategy I: The manipulator is responsible for the fault tolerance. Therefore, from (21) and (22)

$${}^2\mathbf{u} = \left({}^2\mathbf{A}\right)^\dagger\mathbf{a}_2\tau_2 \tag{43}$$

$$\Delta\tilde{\mathbf{f}} = \left(\mathbf{I} - {}^2\mathbf{A}\left({}^2\mathbf{A}\right)^\dagger\right)\mathbf{a}_2\tau_2 \tag{44}$$

Using the values of the parameters that were indicated in Sect. 5.1 results in ${}^2\mathbf{u} = [-36.82 \ -70.43]^T$ and the total-force-jump is $\Delta\tilde{\mathbf{f}} = [0_N \ 0_N]^T$. The fault-tolerant force is achieved because the manipulator is a redundant manipulator and even the faulty manipulator has 2DoF that can tolerate the failure. The post failure human force would be ${}_h\tilde{\mathbf{f}} = [5_N \ 10_N]^T$ equal to that of human prior to the failure.

Test of Strategy II: The human is responsible for the fault tolerance, therefore using (24) the required human force is

$${}_h\tilde{\mathbf{f}} = {}_h\mathbf{f} + \mathbf{a}_2\tau_2 \tag{45}$$

Using the values of the parameters that were indicated in Sect. 5.1 results in ${}_h\tilde{\mathbf{f}} = [22.25_N \ 73.50_N]^T$. However, the human force is limited to $[20_N \ 20_N]^T$. Therefore, the human would apply ${}_h\tilde{\mathbf{f}} = [20_N \ 20_N]^T$ and the total-force-jump would be $\Delta\tilde{\mathbf{f}} = [2.25_N \ 53.50_N]^T$. The post failure force of the manipulator will be ${}_m\tilde{\mathbf{f}} = [27.75_N \ 6.50_N]^T$.

6.3 Test of the Cooperative Strategies

Test of Strategy III: The manipulator maximally tries to resolve the fault, and if any force-jump remains, then the human contributes. For this strategy using (25)

$${}^2\mathbf{u} = -\left({}^2\mathbf{A}\right)^\dagger\mathbf{a}_2\tau_2 \tag{46}$$

Table 4 Human and manipulator force cooperation—third strategy

Joint No	Joint-torque	Force-jump at fault time	Manipulator force	Human force	Force-jump
1	−59.55	$\begin{bmatrix}37.25_N\\63.50_N\\0_N\end{bmatrix}$	$\begin{bmatrix}45_N\\70_N\\0_N\end{bmatrix}$	$\begin{bmatrix}5_N\\10_N\\0_N\end{bmatrix}$	$\begin{bmatrix}0_N\\0_N\\0_N\end{bmatrix}$
2	Locked				
3	−87.22				

Table 5 Human and manipulator force cooperation—forth strategy

Joint No	Joint-torque	Force-jump at fault time	Manipulator force	Human force	Force-jump
1	−44.77	$\begin{bmatrix}17.25_N\\63.50_N\\0_N\end{bmatrix}$	$\begin{bmatrix}30_N\\60_N\\0_N\end{bmatrix}$	$\begin{bmatrix}20_N\\20_N\\0_N\end{bmatrix}$	$\begin{bmatrix}0_N\\0_N\\0_N\end{bmatrix}$
2	Locked				
3	−71.60				

The human force is obtained from (26)

$$ {}_h\tilde{\mathbf{f}} = {}_h\mathbf{f} + \left(\mathbf{I} - {}^k\mathbf{A}\left({}^k\mathbf{A}\right)^{\dagger}\right)\mathbf{a}_k\tau_k \tag{47} $$

Using the values of the parameters that were indicated in Sect. 5.1 results in ${}^2\mathbf{u} = [-36.82\ \ -70.43]^T$ and ${}_h\tilde{\mathbf{f}} = [0_N\ 0_N]^T$, the results are shown in Table 4.

Test of Strategy IV: The human maximally tries to tolerate the fault, if any force remains, then it has to be provided by the manipulator. The results of this strategy are indicated in Table 5.

Test 1 of Strategy V: The human and the manipulator cooperatively contribute to the fault tolerance using a decision making process. Let's assume that the decision-making assigns $\mathbf{W}_m = \mathbf{W}_h = 0.5\mathbf{I}$ where the manipulator is expected to tolerate half of the force-jump and the human the other half. This test is based on (31) and (32) as

$$ {}_h\tilde{\mathbf{f}} = {}_h\mathbf{f} + {}_h\mathbf{W}\mathbf{a}_2\tau_2 \tag{48} $$

$$ {}_m\tilde{\mathbf{f}} = {}_m\hat{\mathbf{f}} + {}_m\mathbf{W}\mathbf{a}_2\tau_2 \tag{49} $$

This gives ${}_h\tilde{\mathbf{f}} = [13.63_N\ 41.75_N]^T$ but the human force is limited to ${}_h\tilde{\mathbf{f}} = [13.63_N\ 20_N]^T$. The result of this test is indicated in Table 6.

In this test, because the manipulator is redundant, therefore the first condition of the zero force-jump in (38) is satisfied, but the human force is out of the bound, therefore a total-force-jump will remain. The force-jump is due to the wrong assignment of $\mathbf{W}_m = \mathbf{W}_h = 0.5\mathbf{I}$.

Test 2 of Strategy V: If the decision-maker assigns $\mathbf{W}_m = \mathbf{I}$ and $\mathbf{W}_0 = 0$ then the force-jump is required to be maximally compensated by the manipulator. This should result in the same outcome as that of the test in strategy I. The results of this case study are shown in Table 7.

Table 6 human and manipulator force cooperation—fifth strategy where $\mathbf{W}_m = \mathbf{W}_h = 0.5\mathbf{I}$

Joint No	Joint-torque	Force-jump at fault time	Manipulator force	Human force	Force-jump
1	−41.17	$\begin{bmatrix}17.25_N\\63.50_N\\0_N\end{bmatrix}$	$\begin{bmatrix}36.37_N\\38.25_N\\0_N\end{bmatrix}$	$\begin{bmatrix}13.63_N\\20_N\\0_N\end{bmatrix}$	$\begin{bmatrix}0_N\\21.75_N\\0_N\end{bmatrix}$
2	Locked				
3	−52.01				

Table 7 human and manipulator force cooperation—fifth strategy $\mathbf{W}_m = \mathbf{I}, \mathbf{W}_h = \mathbf{0}$

Joint No	Joint-torque	Force-jump at fault time	Manipulator force	Human force	Force-jump
1	−59.545	$\begin{bmatrix}17.25_N\\63.50_N\\0_N\end{bmatrix}$	$\begin{bmatrix}45_N\\70_N\\0_N\end{bmatrix}$	$\begin{bmatrix}5_N\\10_N\\0_N\end{bmatrix}$	$\begin{bmatrix}0_N\\0_N\\0_N\end{bmatrix}$
2	Locked				
3	−87.22				

6.4 Discussion

It was mentioned earlier that there is a consistency between the proposed strategies. The consistency is clearly observed in the test of the strategies. The manipulator is a 3DoF planar, and it is not in a singular configuration. Therefore, if a failure occurs, the manipulator is capable of the fault tolerance. This is observed from the results of the tests of the strategies I and III and the second test of V.

If the responsibility of the fault tolerance is assigned to the human as was the case of strategies II and test 1 of strategy IV, then the limit of the human force prevented achieving the complete fault tolerance. In strategy II, this limitation has resulted in a force-jump. In test 1 of strategy V, a non-zero force-jump occurred because of the wrong assignment of the force to the human. In both cases, the assigned force to the human is more than the maximum human force.

7 Simulation Study

Work partner (Wopa) robot has been proposed as a service robot [4], or as an assistant to astronauts [5]. Figure 3 shows the Wopa robot in a load lifting task.

These kinds of robot are assumed to work in close proximity to humans and even in collaboration with humans.

7.1 Simulation Scenario and Parameters

Figure 4 indicates the force cooperation scenario between these robots and humans. The human and the arm of the Wopa robot are applying a force to lift an object. The weight of the object is 80 N. The object needs to be lifted by 0.5 meters in the z direction with a very slow speed. The operator

Fig. 3 Wopa in a lifting scenario [4]

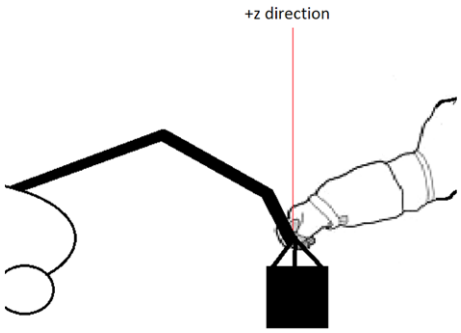

Fig. 4 Human and Wopa arm cooperation

helps the robot by applying 5 N. A locked joint failure is considered for the first joint. It is also assumed that the arm is a 3DoF planar robot moving solely in the XZ plane. The D-H parameters of the robot are shown in Table 1.

7.2 Simulation of the Healthy Wopa Arm

The robot is required to move in the z direction. It is possible to obtain the joint profiles using an iterative inverse kinematics process.

Figure 5 shows the joint profiles that result in 0.5 meters low speed EEF motion in the z direction of the healthy arm. In order to show this, Fig. 6 indicates four snapshots of the configuration of the arm.

Where in Fig. 5, HM indicates the joint profile of the healthy arm and FM indicates the joint profile of the faulty

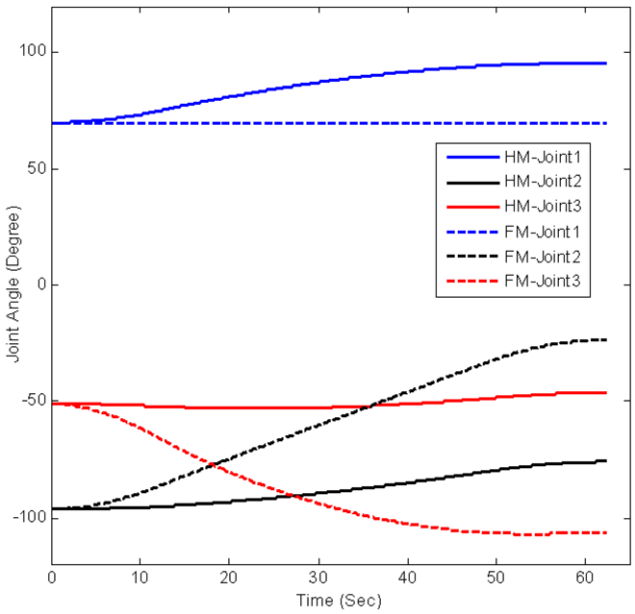

Fig. 5 The joint profiles of the healthy arm (HM) and the joint profiles of the faulty manipulator (FM)

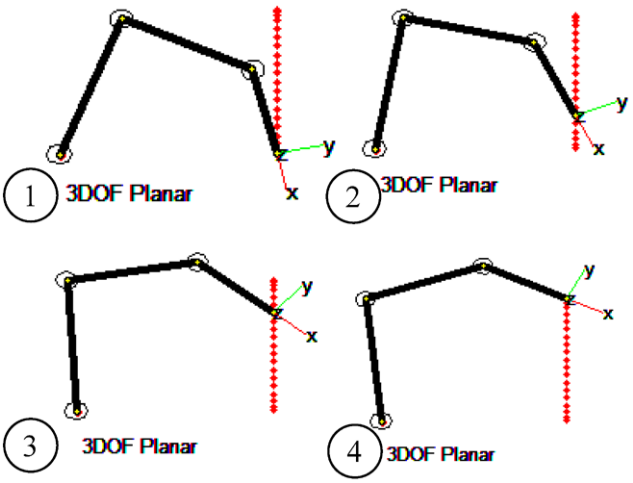

Fig. 6 Four snapshots of the healthy Wopa arm

arm. The method to obtain the joint profiles of the faulty arm will be explained later in this section.

7.3 Simulation of the Faulty Wopa Arm

A failure is assumed to occur in the first joint of the arm.The fault-tolerant HRC requires fault-tolerant motion as well as fault-tolerant force.

7.3.1 Fault-Tolerant Motion of the Arm

The fault-tolerant motion for the arm can be implemented by using the method in [26, 27] that is based on the reconfigu-

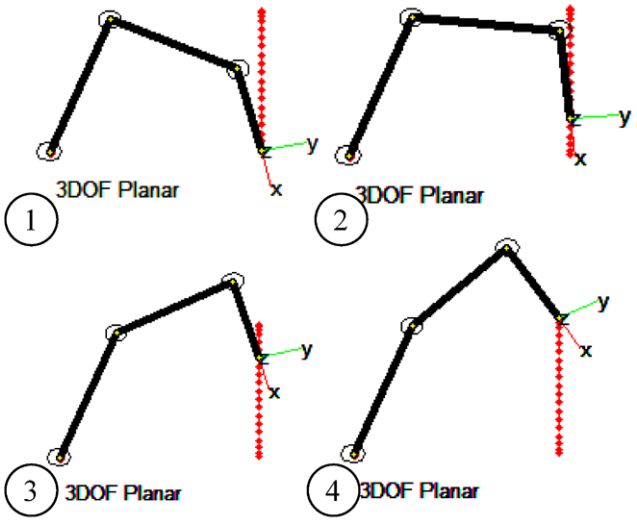

Fig. 7 Four snapshots of the faulty Wopa arm

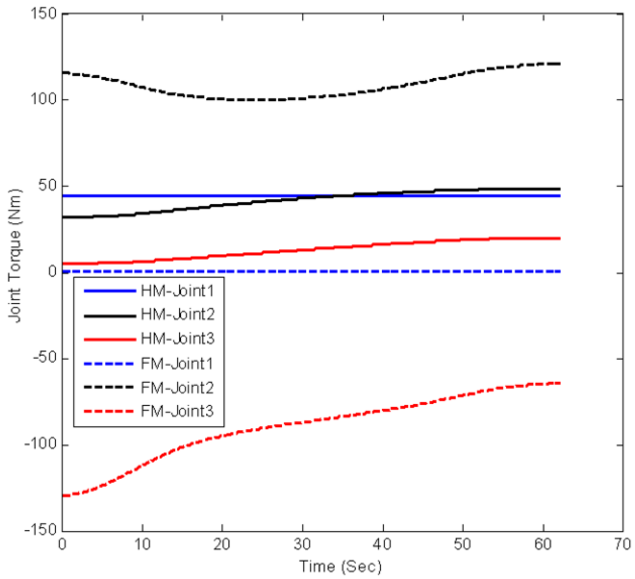

Fig. 8 The joint-torque profiles of the healthy arm (HM) and for the faulty arm (FM) when the first strategy has been employed

ration of the joint velocities. Using this method, the appropriate joint velocities have been obtained as shown in Fig. 5. If the faulty arm joint profiles are applied to the joints, then the EEF will move on the similar path as that of the healthy arm. Figure 7 indicates four snapshots of the configuration of the faulty arm where the first joint is locked and the same path as that of Fig. 6 is obtained.

7.3.2 Fault-Tolerant Force of HRC

The joint torque profiles of the healthy Wopa arm for the EEF force of $[0\ 75_N]^T$ are shown in Fig. 8. The corresponding healthy arm's EEF force is indicated in Fig. 9. The force

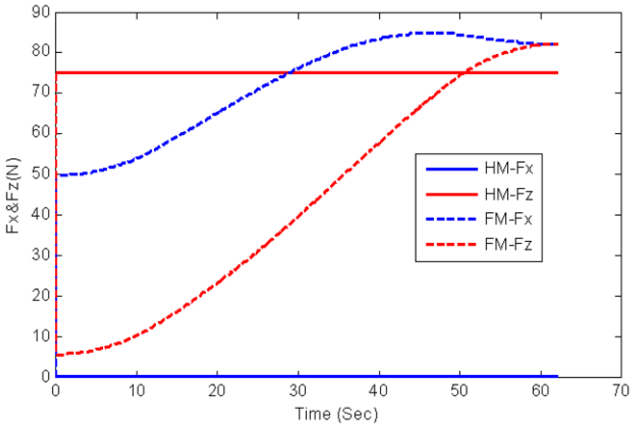

Fig. 9 EEF force of the healthy arm(HM) and the faulty arm(FM), no fault tolerance strategy is used

has two components of Fx and Fz; the y component of the force is always zero because the manipulator is planar. When the arm's first joint fails, the faulty joint torque will be zero. Therefore, the EEF force will change.The force at the EEF after the failure of a joint is indicated in Fig. 9.

The difference between the corresponding healthy and faulty arm's force of Fig. 9 determine the force-jump. This force is for the case that no fault tolerance strategy is employed. In the following subsection the fault tolerance strategies are employed to obtain fault-tolerant force in HRC.

7.4 Simulation Results

Test of Strategy I: The manipulator is responsible for maintaining the force. Therefore, new joint-torque profiles are required to minimize the force-jump. Using strategy 1, the optimal joint-torques are obtained and the results are shown in Fig. 8 by dashed lines.

The EEF force corresponding to these joint torque profiles of the faulty arm is indicated in Fig. 10 showing that the faulty arm is capable of maintaining the force. However, the torques required to maintain the force is large, which can be seen from Fig. 8 and for the torque of the second and third joint.

The difference between the corresponding healthy and faulty arm's force determines the force-jump. The force-jump when strategy 1 was incorporated is shown in Fig. 11 indicating less than 0.3 N force-jump.

Test of Strategy II: If the human is responsible for maintaining the total-force, then the required human force is simply obtained by the difference between the forces prior to the arm's failure and the post failure force. One can simply obtain the required human force by subtracting corresponding forces that were shown in Fig. 9. The required human force for strategy II is shown in Fig. 12.

If the human is able to apply the force of Fig. 12 then the fault is tolerated, otherwise not.

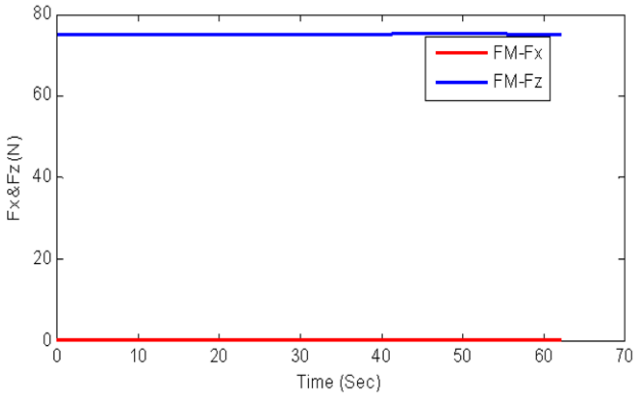

Fig. 10 EEF post failure force of the faulty arm when the strategy I is used

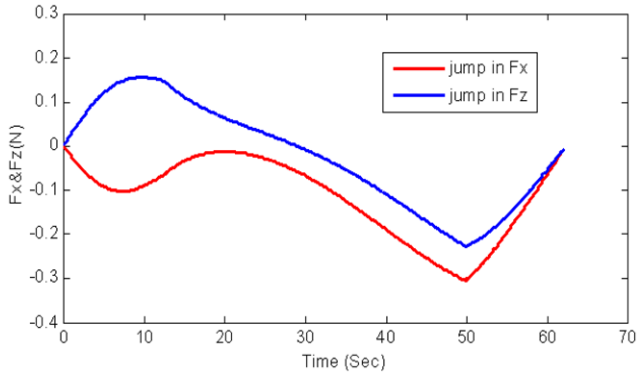

Fig. 11 EEF post failure force-jump of the faulty arm when a strategy as strategy I is applied

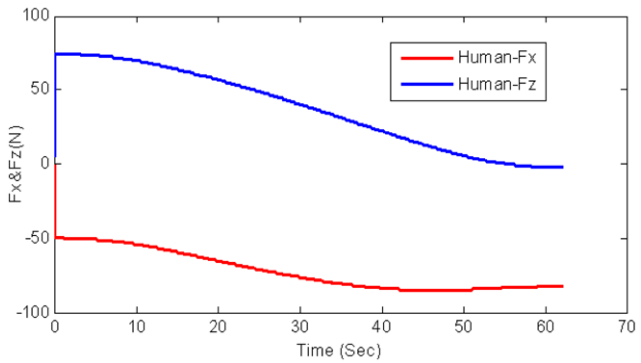

Fig. 12 The required human force as per strategy II

Test of Strategy III: The arm is responsible to optimally tolerate the failure and human would contribute if required. The faulty arm joint-torque profiles and EEF force are the same as that of strategy I shown in Fig. 8, and the EEF force of Fig. 10. Accordingly, the human's reconfiguration force needs to be the force-jump of strategy I. This force-jump was shown in Fig. 11. The required humans force that is shown in Fig. 13 is obtain by adding the force-jump of strategy I to the 5N initial human force.

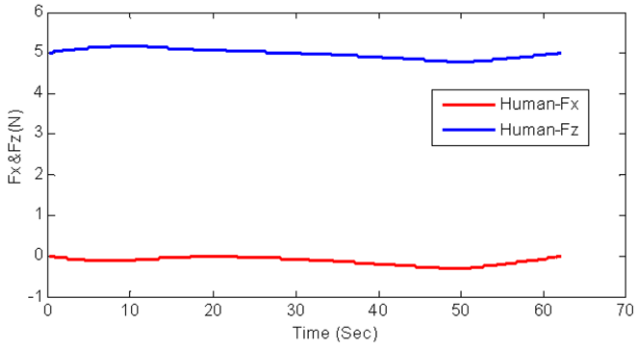

Fig. 13 The required human force of strategy III

Test of Strategy IV: For strategy IV, the result is very similar to that of strategy II. The results will be exactly similar if the human can apply the force that was shown in Fig. 12.

Test of Strategy V: Implementation of strategy V has not been performed because it requires further research to define the decision maker in order to obtain the weight matrices.

Test of the General Strategy: For the general strategy, we observed that it does not provide a uniform way of distributing the force-jump between the human and the faulty manipulator. This is because, at any time instance, the optimization problem exists with multiple global minimum. Then, depending on the initial guess and the method of solving the optimization, different answers will be obtained. For example, for two sequential time instances, it is possible that the force-jump at the first time is assigned mostly to the human and in the second time to the faulty arm. Therefore, the general strategy is not suitable for the simulation study.

Limitations: Every method has some pros and cons; this is also true for the strategies that are presented in this paper. Through the three case studies, we have shown that the strategies are useful for the fault-tolerance in HRC but there are some limitations indicated below.

1. In this paper, the manipulators are positional and we have not considered the orientation of the manipulators. Therefore, the Jacobian matrices are analytical Jacobian matrices. Further work is required to discuss the fault tolerance for spatial manipulators.
2. The strategies are instantaneous. However, via the simulation study, it was shown that the strategies can be used from the time that failure occurs to the end of force task. Therefore, at any time instance after failure up until of the end of the task, the strategies will be applicable.
3. The pseudo inverse method is suitable for local operation. It was used in this paper because we assume the robot's effective workspace is small.
4. Strategy V has not been extensively discussed in detail as it was relying heavily on a decision-making process. The optimal selection of the matrices requires further research.

5. In the present paper, we have discussed that the strategies are for stationary or slow moving cases. Fault tolerant HRC for a fast moving manipulator is not considered because of the safety issues.
6. Another issue is multiple joint failures. We have developed optimal fault-tolerant motion for multiple joint failures of a manipulator in [27]. A similar approach with some modification can be used for fault tolerant force with multiple actuator failures.

8 Conclusion

This work has investigated different strategies for the application of optimal fault-tolerant force within human-robot cooperation for the slow pushing or lifting of an object. Six different strategies were presented to optimally maintain a cooperative force despite manipulator failure through a locked joint event. These strategies determined the post failure cooperation of the faulty manipulator and the human.

The strategies were validated using three case studies. It was indicated that the cooperation strategies not only resulted in a fault-tolerant force when the conditions of full fault tolerance were held, but they also provided consistent results in comparison with each other. The third case study simulated the fault-tolerant cooperative force of a Wopa arm, and a human.

All three case studies indicated the fault-tolerant force of the human and the robot. The present strategies can be applied for robots assisting humans such as surgeons, astronauts, and also the disabled or the elderly.

The contribution in this paper is complementary to the previous work presented for the study of fault-tolerant motion [26, 29], and fault-tolerant force for single and multiple manipulators [25, 30, 31]. This is achieved by extending the fault-tolerant force to human-robot cooperation.

Acknowledgements This research was supported by Centre for Intelligent Systems Research—Deakin University in part with U.S. National Science Foundation under contract IIS-0812437.

Appendix A

The pseudo inverse of full rank square matrices is obtained by regular inverse or

$$\mathbf{B}^{\dagger} = \mathbf{B}^{-1}$$

when $\mathbf{B}$ is a skinny full rank matrix, then the pseudo inverse is defined by left inverse or

$$\mathbf{B}^{\dagger} = \left(\mathbf{B}^{T}\mathbf{B}\right)^{-1}\mathbf{B}^{T}$$

when $\mathbf{B}$ is a fat and full rank matrix, then the pseudo inverse is defined by right inverse or

$$\mathbf{B}^{\dagger} = \mathbf{B}^{T}\left(\mathbf{B}\mathbf{B}^{T}\right)^{-1}$$

Appendix B

Reduced matrices are defined by eliminating columns of the matrices. For example, by eliminating the kth column of $\mathbf{A}$, the kth reduced matrix is obtained as

$${}^{k}\mathbf{A} = \begin{bmatrix} \mathbf{a}_1 & \cdots & \mathbf{a}_{k-1} & \mathbf{a}_{k+1} & \cdots & \mathbf{a}_n \end{bmatrix}$$

Reduced vectors are defined similar to reduced vertices eliminating the rows. The kth reduced vector of $\boldsymbol{\tau}$ is

$${}^{k}\boldsymbol{\tau} = [\,\tau_1 \quad \cdots \quad \tau_{k-1} \quad \tau_{k+1} \quad \cdots \quad \tau_n\,]^{T}.$$

For single locked joint failures, there are n reduced matrices of $\mathbf{A}$ which are shown by ${}^{1}\mathbf{A}, {}^{2}\mathbf{A}, \ldots, {}^{n}\mathbf{A}$.

References

1. Lallee S, Yoshida E, Mallet A, Nori F, Natale L, Metta G, Warneken F, Dominey P (2010) Human-robot cooperation based on interaction learning. In: Sigaud O, Peters J (eds) From motor learning to interaction learning in robots. Studies in computational intelligence, vol 264. Springer, Berlin, pp 491–536
2. López M, Barea R, Bergasa L, Escudero M (2004) A human–robot cooperative learning system for easy installation of assistant robots in new working environments. J Intell Robot Syst 40:233–265
3. Wojtara T, Uchinara M, Murayama H, Shimoda S, Sakai S, Fujimoto H, Kimura H (2009) Human-robot cooperation in precise positioning of a flat object. Automatica 45:333–342
4. Heikkilä S, Halme A, Schiele A (2010) Human-human inspired task and object definition for astronaut-robot cooperation. In: Proc. of the 10th international symposium on artificial intelligence, robotics and automation in space (i-SAIRAS)
5. Bluethmann W, Ambrose R, Diftler M, Askew S, Huber E, Goza M, Rehnmark F, Lovchik C, Magruder D (2003) Robonaut: a robot designed to work with humans in space. Auton Robots 14:179–197
6. Kumar R, Berkelman P, Gupta P, Barnes A, Jensen P, Whitcomb L, Taylor R (2000) Preliminary experiments in cooperative human/robot force control for robot assisted microsurgical manipulation. In: Proceeding of the IEEE international conference on robotics and automation, San Francisco, CA, USA, pp 610–617
7. Kargov A, Asfour T, Pylatiuk C, Oberle R, Klosek H, Schulz S, Regenstein K, Bretthauer G, Dillmann R (2005) Development of an anthropomorphic hand for a mobile assistive robot. In: Proceeding of the IEEE international conference on rehabilitation robotics, Chicago, IL, USA, pp 182–186
8. Koeppe R, Engelhardt D, Hagenauer A, Heiligensetzer P, Kneifel B, Knipfer A, Stoddard K (2005) Robot-robot and human-robot cooperation in commercial robotics applications. Robot. Res., 202—216
9. Yong Y, Lan W, Jie T, Lixun Z (2006) Arm rehabilitation robot impedance control and experimentation. In: Proceeding of the IEEE international conference on robotics and biomimetics, pp 914–918
10. Fong T, Nourbakhsh I, Dautenhahn K (2003) A survey of socially interactive robots. Robot Auton Syst 42:143–166
11. Abdi H, Nahavandi S (2012) Well-conditioned configurations of fault-tolerant manipulators. Robot Auton Syst 60:242–251
12. Haddadin S, Albu-Schäffer A, Hirzinger G (2011) Safe physical human-robot interaction: measurements, analysis and new insights. Springer tracts in advanced robotics, vol 66, pp 395–407

13. Abdi H, Nahavandi S, Masouleh MT (2010) Minimal force jump within human and assistive robot cooperation. In: Proceeding of the IEEE/RSJ international conference on intelligent robots and systems, Taiwan, pp 2651–2656
14. Alami R, Albu-Schaeffer A, Bicchi A, Bischoff R, Chatila R, De Luca A, De Santis A, Giralt G, Guiochet J, Hirzinger G (2006) Safe and dependable physical human-robot interaction in anthropic domains: state of the art and challenges. In: Proceeding of the IEEE/RSJ international conference on intelligent robots and systems, 'Workshop on pHRI—physical human-robot interaction in anthropic domains', pp 1–15
15. Goetz J, Kiesler S, Powers A (2003) Matching robot appearance and behavior to tasks to improve human-robot cooperation. In: Proceeding of the 12th IEEE international workshop on robot and human interactive communication, pp 55–60
16. Yamada Y, Yamamoto T, Morizono T, Umetani Y (1999) FTA-based issues on securing human safety in a human/robot coexistence system. In: Proceeding of the IEEE international conference on systems, man, and cybernetics, pp 1058–1063
17. Kosuge K, Kakuya H, Hirata Y (2001) Control algorithm of dual arms mobile robot for cooperative works with human. In: Proceeding of the IEEE international conference on systems, man, and cybernetics, pp 3223–3228
18. Tsumugiwa T, Yokogawa R, Hara K (2002) Variable impedance control based on estimation of human arm stiffness for human-robot cooperative calligraphic task. In: Proceeding of the IEEE international conference on robotics and automation, San Diego, CA, USA, pp 644–650
19. Takubo T, Arai H, Hayashibara Y, Tanie K (2002) Human-robot cooperative manipulation using a virtual nonholonomic constraint. Int J Robot Res 21:541
20. Harwin WS (2009) Impedance mismatch: some differences between the way humans and robots control interaction forces. In: Proceeding of the IEEE international conference on rehabilitation robotics, p 19
21. Hyowon J, Seul J (2009) Hardware design on an FPGA chip of impedance force control for interaction between a human operator and a robot arm. In: Proceeding of the 7th Asian control conference (ACC), pp 1480–1485
22. Kye-Young L, Seung-Yeol L, Jong-Ho C, Sang-Heon L, Chang-Soo H (2006) The application of the human-robot cooperative system for construction robot manipulating and installing heavy materials. In: Proceeding of the international joint conference SICE-ICASE, pp 4798–4802
23. Lamy X, Colledani F, Gutman PO (2010) Identification and experimentation of an industrial robot operating in varying-impedance environments. In: Proceeding of the IEEE/RSJ international conference on intelligent robots and systems (IROS), pp 3138–3143
24. Minyong P, Mouri K, Kitagawa H, Miyoshi T, Terashima K (2007) Hybrid impedance and force control for massage system by using humanoid multi-fingered robot hand. In: Proceeding of the IEEE international conference on systems, man and cybernetics, pp 3021–3026
25. Abdi H, Nahavandi S (2010) Fault tolerance force for redundant manipulators. In: Proceeding of the IEEE international conference on advanced computer control, pp 612–617
26. Abdi H, Nahavandi S (2010) Joint velocity redistribution for fault tolerant manipulators. In: Proceeding of the IEEE conference on robotics automation and mechatronics, pp 492–497
27. Abdi H, Nahavandi S, Frayman Y, Maciejewski AA (2011) Optimal mapping of joint faults into healthy joint velocity space for fault tolerant redundant manipulators. Robotica. doi:10.1017/S0263574711000671, pp. 1–14
28. Corke PI (1996) A robotics toolbox for MATLAB. IEEE Robot Autom Mag 3:24–32
29. Abdi H, Nahavandi S (2010) Optimal actuator fault tolerance for static nonlinear systems based on minimum output velocity jump. In: Proceeding of the IEEE international conference on information and automation, pp 1165–1170
30. Abdi H, Nahavandi S, Najdovski Z (2010) On the effort of task completion for partially-failed manipulators. In: Proceeding of the IEEE international conference on industrial informatics, pp 201–206
31. Abdi H, Nahavandi S, Najdovski Z (2010) Fault tolerance operation of cooperative manipulators. In: Proceeding of the IEEE international symposium on artificial intelligence, robotics and automation in space, Japan, pp 144–151

Hamid Abdi B.Sc. and M.Sc. degrees in control engineering from EE department in Sharif University of Technology, Iran, and Ph.D. from Deakin University, Australia. From 2000 to 2008, Hamid has worked in the EE department, Iran University of Science and Technology, Arak-Iran. Hamid has received several awards including Sharif University vice chancellor award 2 times, minister of petroleum award, and minister of science and technology certificate. He also has received the UNESCO entrepreneurship award and certificate and a golden medal of Sheikh Baha'i for his innovative robot for traffic control and road safety. Hamid has been selected in the top ten researchers among academic and research staffs, in Markazi-Iran. Hamid's research interests include advanced industrial control, fault-tolerant systems, robot kinematics and dynamics, and energy saving.

Saeid Nahavandi (SM'07) received B.Sc. (hons.), M.Sc., and Ph.D. degrees in automation and control from Durham University, Durham, U.K. He is an Alfred Deakin Professor, Chair of Engineering, and the Director for the Intelligent Systems Research Centre, Deakin University, Geelong, VIC, Australia. He has published over 450 peer reviewed papers in various international journals and conferences. He designed the world's first 3-D interactive surface/motion controller. His research interests include modeling of complex systems, simulation-based optimization, robotics, haptics and augmented reality. Saeid is the Associate Editor of the IEEE SYSTEMS JOURNAL, an Editorial Consultant Board member for the International Journal of Advanced Robotic Systems, an Editor (South Pacific Region) of the International Journal of Intelligent Automation and Soft Computing. He is a Fellow of Engineers Australia (FIEAust) and IET (FIET).

Zoran Najdovski received BEng (Hons) and BSci in Mechatronics and Software Development and PhD in Haptics from Deakin University (Australia). He is currently a research fellow within the Centre for Intelligent Systems Research at Deakin University, Australia. His research interests include the control and analysis of haptic interfaces and their contribution to human haptic perception, development of novel haptic interface devices, and robotics modeling and control.

Anthony A. Maciejewski (M'87–SM'00–F'05) received B.S.E.E., M.S., and Ph.D. degrees from Ohio State University, Columbus, in 1982, 1984, and 1987, respectively.
From 1988 to 2001, he was a Professor of electrical and computer engineering at Purdue University, West Lafayette, IN. He is currently the Department Head of Electrical and Computer Engineering at Colorado State University, Fort Collins.